Proc Nat. Acad. Sci. USA
Vol. 68, No. 12, pp. 3000-3004, December 1971

Visualization of Single Heavy Atoms by Dark Field Electron Microscopy

(electron scattering cross-section/carbon film/uranium atom/self-consistent field wave functions)

R. M. HENKELMAN AND F. P. OTTENSMEYER

Department of Medical Biophysics, University of Toronto, and the Ontario Cancer Institute, 500 Sherbourne Street, Toronto, Canada

Communicated by Norman Davidson, September 24, 1971

ABSTRACT **Dark field electronmicrographs of atoms of palladium, iodine, platinum, osmium, and uranium in model compounds have been obtained. Statistical analyses and a series of blind tests demonstrate the validity of the results. Moreover, optical density measurements of the images indicate that the observed relative scattering cross-sections of these atoms agree well with the theoretical cross-sections calculated from a Thomas–Fermi–Dirac model of the atom.**

The visualization of single atoms has long been a goal of electron microscopy—a goal that the increased resolving power of modern microscopes of conventional design and the development of new kinds of microscopes are beginning to achieve. As early as 1957, Mueller (1) observed atoms in single crystal metal tips using field ion microscopy. However, the biologist interested, for instance, in analyzing the base sequence of nucleic acids by the use of heavy atom markers, requires that isolated single heavy atoms be imaged. Up to the present, the only technique capable of this has been transmission scanning electron microscopy of high resolution, in conjunction with electron energy analysis (2), although a recent report by Koller (3) indicates that it may be possible to image heavy atoms by the use of traditional brightfield transmission electron microscopy. One of the principal difficulties in the use of a conventional electron microscope for the visualization of atoms has been the lack of contrast. Even though the scattering of a single heavy atom can be shown theoretically to produce a reasonable variation in the intensity of the electron beam that produces the electronmicrograph, when the atom is supported on a substrate film, the image signal of the atom is extremely difficult to differentiate from the random fluctuations of the background caused by electron noise, support-film irregularities, and, to a smaller extent, photographic grain.

In this paper, the use of dark field electron microscopy is proposed to overcome the contrast problem. It is shown that dark field conditions produce much improved contrast for heavy atoms, although longer exposure times are required. Dark field electronmicrographs of such atoms are presented, and the images are analyzed statistically and densitometrically and are compared with the relative theoretical electron-scattering intensities for the atoms observed. The results, including atoms ranging over the upper half of the periodic table incorporated in different model molecules and in DNA, indicate that single atoms are visualized. While the applications of this technique are many, our aim is to use it in the sequence determination of nucleic acid bases by the use of specific heavy atom markers.

Abbreviation: TFD model, Thomas–Fermi–Dirac model.

COMPARISON OF BRIGHT FIELD AND DARK FIELD ELECTRON MICROSCOPY FOR THE VISUALIZATION OF HEAVY ATOMS

If one considers a single uranium atom on a thin carbon film, a comparison can be made of the contrast obtained in the electron images of such an atom in the bright field and dark field modes of operation of the electron microscope. For this, one has to obtain the fraction of the incoming electrons scattered by the carbon film and also by the uranium atom, outside the objective aperture of the instrument in bright field conditions and into the aperture in dark field. In our case, an objective aperture with an angular radius of 8.6×10^{-3} radians was placed in the back focal plane of a standard Philips EM300 microscope operating at 80 kV. For dark field conditions, the incident electron beam was tilted 1.3×10^{-2} radians (about 0.75°), so that all of the incident electrons were stopped by the edge of the aperture.

The thin carbon film supporting the heavy atoms was produced by indirect evaporation, a method described elsewhere (Whiting and Ottensmeyer, submitted for publication). By weighing 10 films of known area and using a density of 1.9 g/cm^3 for amorphous carbon, we determined the film thickness [2 ± 0.5 nm (20 ± 5 Å)]. Since the scattering of electrons from such films is known to have interference effects and is therefore not in exact agreement with a single-atom theory over large angles, the fraction of electrons scattered by the carbon film, or effectively its differential scattering cross-section, was determined experimentally from the carbon film diffraction pattern. To cover the large range of intensities, the pattern was recorded on Electron Image Plates (Kodak) with exposures ranging from 0.125 to 64 sec. The intensities were measured by a Joyce Loebl Recording Microdensitometer MK IIICS. The somewhat nonlinear response of the photographic emulsion necessitated a careful calibration and correction, whereupon the scattering intensities recorded at different exposures became colinear over the entire range to 0.1 radians. Analysis of the curve indicated excellent agreement with the experimental work of Bruenger and Menz (4) and with the theoretical single carbon atom cross-section of Burge, Misell, and Smart (5) at small angles. For bright field conditions (central placement of the diffraction pattern with respect to the objective aperture), the scattering by the carbon film outside the objective aperture was found to be 3.1% of the incoming beam, while for dark field (1.3×10^{-2} radian dis-

placement of the diffraction pattern), the scattering into the aperture was 0.57% of the incoming beam. This determines the background levels indicated in Fig. 1.

The scattering of a uranium atom is predominantly elastic. Therefore the elastic differential cross-section as calculated from a Thomas–Fermi–Dirac (TFD) model of the atom (6) may be used to calculate the number of electrons scattered by the uranium atom. (Although the statistical TFD model of the atom is relatively undetailed, it is expected that the use of the recent Hartree-Fock self-consistent field wavefunctions of the atom would give answers differing by only a few percent. The relatively large (about 20%) variances observed in the experimental measurements made the use of the more complicated wave-functions unjustifiable.) In the image, the electrons scattered from the uranium atom are assumed to be focussed into a Gaussian shaped image with a width of 0.2 nm (2 Å). This is in agreement with the theoretical resolution calculated by Koike and Kamiya (7) and by Crick and Misell (8). The results are summarized in Fig. 1. It can be seen that although axial illumination (bright field condition) gives a large signal for the uranium atom (10.5% of the incoming beam), it is only 11% of the background. This is extremely close to the limit of detection, which is accepted to be between 5 and 10% (9). However, in the case of tilted illumination (dark field condition) the signal, although as small as 0.64% of the incoming beam, is 112% of the background, a 10-fold increase in contrast over bright field conditions and well above the detectable limit. Moreover, while in bright field operation the contrast is virtually independent of the support thickness, it can even be increased by use of a thinner support in dark field. We therefore conclude that while it would be possible to detect heavy atoms in bright field operation, it should be much easier to do so in dark field.

Contrast, however, is not the only consideration in the observation of atoms. While sufficient contrast in the image must exist to make the atoms observable at all, random fluctuations in the background must be small enough not to

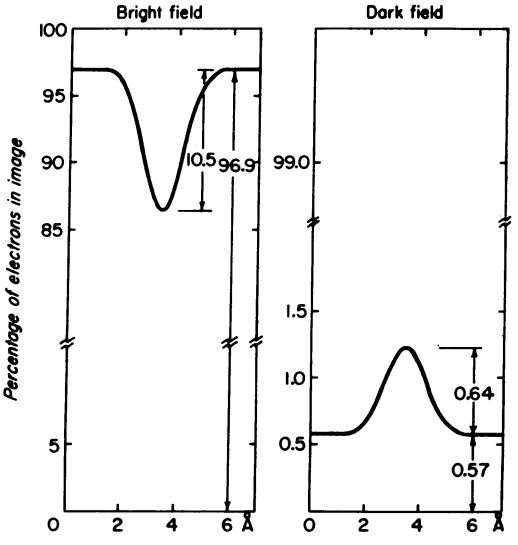

FIG. 1. The theoretically predicted image contrast for a uranium atom supported on a 2-nm (20-Å) thick amorphous carbon film. The contrast is 10 times greater in the dark-field image, even though the total intensity in the atom image is decreased almost 20-fold.

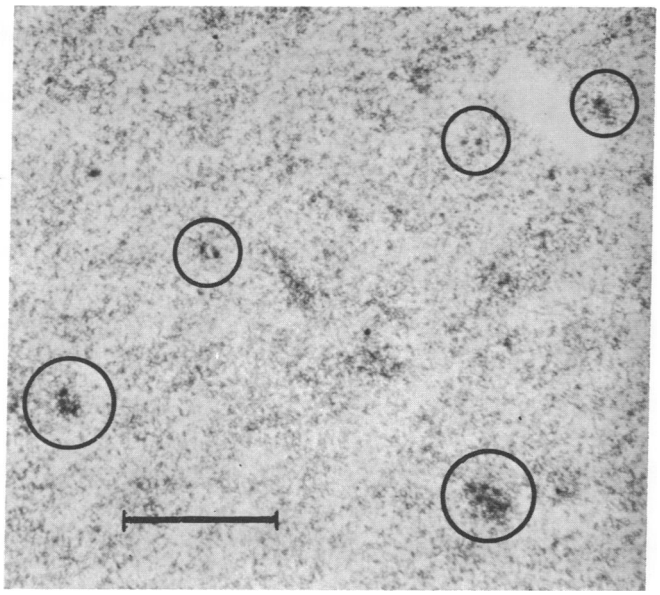

FIG. 2. Dark-field image of carbon film supporting planar molecules of di-tetramethylammonium-di-μ-iodo-tetraiododi-platinum(II), containing two platinum atoms with a spacing of about 0.4 nm (4 Å). Pairs or clusters of pairs of dots can be seen in the *encircled areas* of the electron micrograph. The range of densities in this print has been reduced by the use of an unsharp filter (12). The bar represents 5 nm (50 Å).

interfere with the image signal. Part of these fluctuations are introduced by photographic recording and by the statistical accumulation of the electrons that form the image. However, calculations by Siegel (10) show that such fluctuations are small enough to image a 0.2-nm (2-Å) atom satisfactorily at an electron optical magnification of 100,000. The results presented in this paper bear this out.

Last, the effect of the 30-fold or greater increase in exposure of the specimen required in dark-field operation must be considered. Certainly, a complex biological specimen would be expected to be damaged (11); however, single heavy atoms cannot be damaged. There is only the risk of their movement during the exposure. Even so, such movement is minimized by the large mass of the atom. Nevertheless, exposure times were kept as short as possible for all electronmicrographs by performing all instrumental adjustments on an area adjacent to the one photographed.

RESULTS AND DISCUSSION

Fig. 2 is a dark field electronmicrograph of a thin carbon film that contains molecules of di-tetramethylammoniumdi-μ-

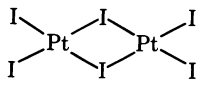

iodotetraiodo-diplatinum(II). The heaviest atoms in these molecules are two covalently bound platinum atoms. Despite the granularity of the background, pairs of black dots and clusters of pairs with a spacing of about 0.4 nm (4 Å) stand out clearly. The spacing corresponds to that of the platinum atoms in the molecule, suggesting strongly that the pairs of dots may be identified as the platinum images. Five other model molecules containing iodine, palladium, osmium, platinum, or uranium atoms have been studied as well (Whiting and

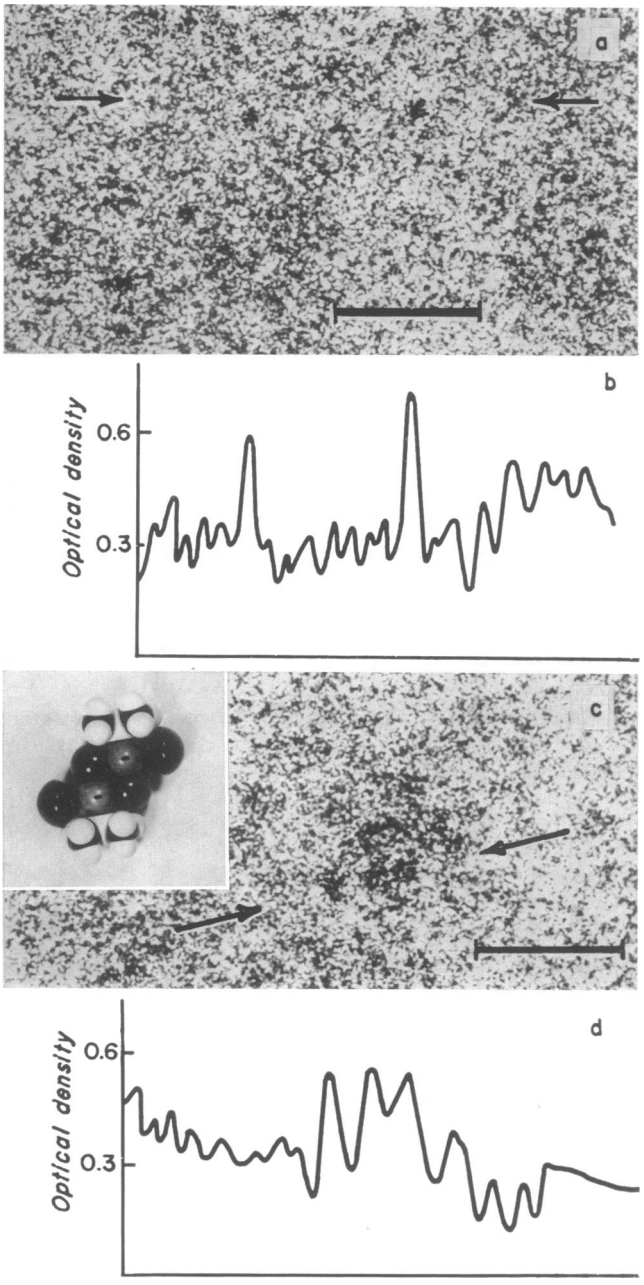

FIG. 3. Dark-field images (*a*) of osmium atoms attached to thymine moieties in single-stranded DNA of bacteriophage ϕX174, and (*c*) of a molecule of an iodine-palladium-bridged dimer, showing a very clear iodine-palladium-iodine row of atoms. The model of the molecule is shown in the *insert*. In contrast to Fig. 2, the prints here reflect the full range of densities observed on the original image plate. (*b*) and (*d*) show densitometer traces made on the original image plates in the regions depicted in the micrographs above them. The line of the trace is indicated by the *arrows* in the micrographs. The bars represent 1 nm (10 Å).

Ottensmeyer, submitted for publication). In each of these molecules, there was excellent qualitative agreement between the images and the configuration and spacing of the atoms in the molecules. Moreover, for molecules that contained more than one type of heavy atom, the images of the heavier atoms appeared darker. This observation suggested a quantitative comparison of the photographically recorded electron-scattering intensity for a given atom with the theoretically expected scattering under dark-field conditions.

The darkening of the images of four types of atoms—palladium, iodine, osmium, and uranium—was measured densitometrically on the original plates (Electron Image Plates, Kodak) by a Joyce Loebl Recording Microdensitometer MK IIICS with a square effective spot of 100 μm^2. This spot corresponded to 0.01 nm^2 (1 $Å^2$) in the original specimen. Measurements were made of the peak atom density and of the background density in the immediate vicinity of the atom image. Since we could not determine accurately the integrated density of the electrons scattered by the atom into the image, the peak optical density, proportional to the integrated density for Gaussion distributions of constant half-widths, was taken to be representative of the total electron scatter. Typical density traces across atom images are shown in Fig. 3*b* for two osmium atoms selectively attached to thymine in purified, single-stranded DNA of bacteriophage ϕX174, and in Fig. 3*d* for an iodine–palladium–iodine row in an iodine–palladium-bridged dimer molecule [sym-trans-di-μ-iodo-diiodobis(dimethylphenylarsine)dipalladium(II)]. The corresponding images are shown above the traces (for experimental procedures on these molecules, see Whiting and Ottensmeyer, submitted for publication). The results of these measurements are summarized in Table 1.

In this Table, the measured photographic density for atom and support is shown in columns 3 and 4. To correspond to electron-scattering intensities, these values have to be corrected for the nonlinear emulsion response of the recording plates. The "Observed Relative Scattering Intensity" for a given atom is the ratio of corrected density of the net signal to the corrected density of the support. In this ratio, the ob-

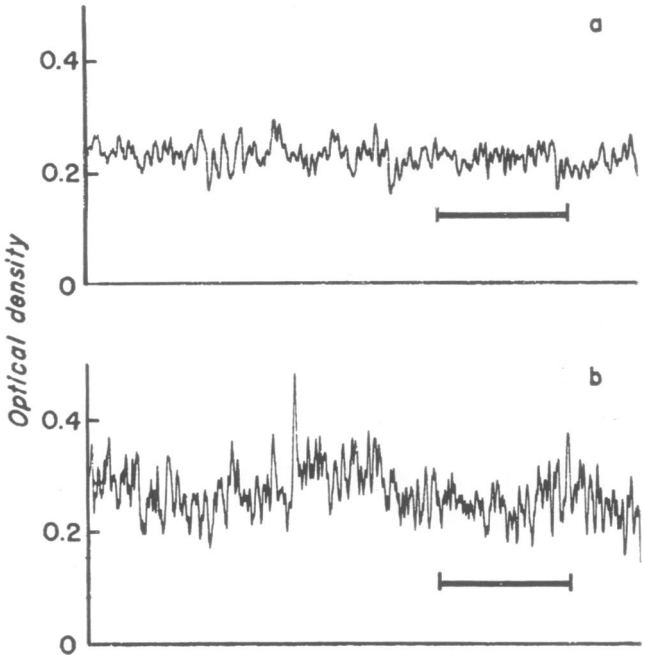

FIG. 4. (*a*) Optical density trace of an Electron-Image Plate, exposed by a uniform electron beam, shows noise due to film grain and the stochastic nature of electron imaging. (*b*) Optical density trace of the dark field image of a carbon film supporting single-stranded ϕX174 DNA that is osmium-stained. The obvious large spike is due to an osmium atom. The bars represent 5 nm (50 Å).

TABLE 1. *Observed and expected ratios for heavy atoms relative to the carbon support*

Atom	Atomic number	Measured density*		Relative scattering intensity	
		Net signal	Support	Observed	Expected
Pd	46	0.18 ± 0.05	0.29 ± 0.05	0.71 ± 0.38	0.75
I	53	0.22 ± 0.04	0.29 ± 0.05	0.87 ± 0.28	0.90
Os	76	0.34 ± 0.05	0.30 ± 0.03	1.23 ± 0.30	1.42
U	92	0.26 ± 0.04	0.16 ± 0.05	2.07 ± 0.85	1.81

* The measured density is that obtained by the densitometer from the original electron-image plates. The observed relative scattering is the measured net signal divided by the support, including a correction for the nonlinear response of the image plates. A description of the theoretically predicted relative scattering intensity is included in the text.

served electron-scattering intensities of the different atoms are effectively normalized to a carbon film of constant thickness. To obtain the "Expected Relative Scattering Intensities," the theoretical differential scattering cross-sections for the atoms were calculated for dark field conditions under the assumptions that the thickness of the carbon support film and the size of the atomic image are constant for the series of measurements. The latter is a justifiable assumption when it is realized that the image size is primarily due to the resolving power of the instrument. The calculated cross-sections were then each multiplied by the same constant to obtain the values in column 6. The constant was chosen to give the best fit through the experimentally observed values. The agreement between the observed and expected values is excellent, even though the atoms range in atomic number over half of the periodic table and the images were obtained from molecules on different carbon films and at different times. The differences still seen could easily be due to differences in carbon film thickness of the order of 10–15%, or differences in the resolving power of the electron microscope of 5–7% incurred during the alignment of the instrument.

Nevertheless, since the variances on the observed contrast values were of the order of 25–50%, the possibility of observing molecular configurations at random was investigated. From densitometer traces of photographic plates exposed by a uniform electron beam (e.g., Fig. 4*a*), it was found that the variance of electron noise plus film grain was 0.025 at an optical density of 0.3, increasing slightly to about 0.04 at an optical density of 1.5. The total variance observed in dark field images of carbon films with or without additional heavy atoms (trace in Fig. 4*b*) was at most 0.05, or twice the variance of electron noise and film grain alone.

By use of the total observed variances for the carbon support shown in Table 1, column 4, the calculated probability of finding a spot as dark as those representing iodine or palladium is about 0.00032 per 100 μm^2 on the photographic plate. Therefore, the probability of finding even one configuration such as the iodine–palladium-bridged dimer shown in Fig. 3*a* on an entire 10.6 × 13.1 cm (4.25 × 5.25 inches) photographic plate at random is less than 0.0001. The observation of about five such molecules per cm^2 and about 50 less-perfect, but nevertheless recognizable, structures in the same area, makes their random occurrence extremely unlikely.

To further validate the results, several types of blind and double-blind tests were performed. All tests performed by persons who have some experience with dark field images were highly significant. Even the most stringent test, a double-blind test involving an outside referee and a subject who had had no experience with electron microscopic images, was very significant. In this test, the referee was given a series of numbered but otherwise unmarked original electron-image plates of dark field images, of empty carbon films, or of films containing nine different molecules, including atomic specimens, as well as such molecules as transfer RNA or RNase. Five of these plates were selected by the referee, the numbers were covered, replaced by letters, and given to the subject for identification. The subject correctly identified plates containing images of molecules of the iodine–palladium-bridged dimer shown in Fig. 3*c*, molecules of uranyl-stained 1,2,4-benzenetricarboxylic acid, and a plate of images of *N*-formylmethionyl transfer-RNA. Considering the 10 possible choices for each trial, the probability of obtaining this result at random is 0.008. On this same test, our experienced observer, in addition, correctly identified plates containing images of RNase and an empty carbon film. The probability of obtaining this result at random is 0.00001.

SUMMARY

Theory indicates that the contrast in the image of a uranium atom on a thin carbon film is 10 times greater in dark field images than in bright field images. In practice, however, a noisy background contributes considerably to the difficulties in visualizing such an atom. Nevertheless, dark field images of molecules were observed in which the configuration and spacing of dots in the image corresponded directly to the configuration and spacing of atoms in the molecules. Moreover, the observed scattering cross-sections for atoms widely spaced in the periodic table of elements were found to be directly related to the theoretically calculated cross-sections for these atoms. The possibility of chance occurrences of the configurations, such as those observed, was eliminated by a statistical analysis of carbon-film images as well as by a series of blind tests. We conclude, therefore, that heavy atoms have been visualized by dark-field transmission electron microscopy.

We thank Dr. G. F. Whitmore for his assistance in the blind tests and the Hamilton Health Department for the use of the densitometer. R.M.H. held a University of Toronto Open Fellowship. This work was supported by the National Cancer Institute of Canada and Grant MA-3763 from the Medical Research Council of Canada.

1. Mueller, E. W., *J. Appl. Phys.*, **28**, 1 (1957).
2. Crewe, A. V., J. Wall, and J. Langmore, *Science*, **168**, 1338 (1970).
3. Koller, T., *Biophys. J.*, **11**, 216a (1971).
4. Bruenger, W., and W. Menz, *Z. Phys.*, **184**, 271 (1965).

5. Burge, R. E., D. L. Misell, and J. W. Smart, *J. Phys. C*, **3**, 1661 (1970).
6. *International Tables for X-ray Crystallography* (Kynoch Press, Birmingham, 1962), Vol. 3, p. 221, Table 3.3.3.A(2).
7. Koike, H., and Y. Kamiya, *Septieme Congres International de Microscopie Electronique* (Grenoble, 1970), Vol. 1, p. 27.
8. Crick, R. A., and D. L. Misell, *J. Phys. D*, **4**, 1 (1971).
9. Heindenreich, R. D., in *Fundamentals of Transmission Electron Microscopy*, ed. R. E. Marshak (Interscience Publishers, New York, 1964), p. 31.
10. Siegel, B. M., in *Modern Developments in Electron Microscopy*, ed. B. M. Siegel (Academic Press, New York, 1964), p. 71.
11. Breedlove, J. R., and G. T. Trammel, *Science*, **170**, 1310 (1970).
12. Hamilton, J. F., *J. Appl. Phys.*, **39**, 5333 (1968).